The theoretical charge density of silicon: experimental testing of exchange and correlation potentials

1997 J. Phys.: Condens. Matter 9 7541

(http://iopscience.iop.org/0953-8984/9/36/004)

J. Phys.: Condens. Matter **9** (1997) 7541–7561. Printed in the UK PII: S0953-8984(97)83633-8

The theoretical charge density of silicon: experimental testing of exchange and correlation potentials

J M Zuo†§, P Blaha‡ and K Schwarz‡

† Department of Physics and Astronomy, Arizona State University, Tempe, AZ 85287, USA
‡ Institut für Technische Elektrochemie der Technischen Universität, Wien, Austria

Received 21 April 1997, in final form 13 June 1997

Abstract. 31 highly accurate, experimentally measured, structure factors of silicon for reflections from (111) to (880) are used to test various approximations for exchange and correlation potentials. Specifically, the Hartree–Fock method and some of its extensions, and the density functional theory in the local density approximation (LDA), and two newly developed refinements, namely the generalized gradient approximations (GGAs) of Perdew and Wang (Perdew J P, Chevary J A, Vosko S H, Jackson K A, Pederson M R, Singh D J and Fiolhais C 1992 *Phys. Rev.* B **46** 6671) and Engel and Vosko (Engel E and Vosko S H 1993 *Phys. Rev.* B **47** 13 164) are used. The multi-configuration Hartree–Fock method including relativistic effects gives the best description of the core electron densities. The charge density calculated with the GGA of Perdew and Wang leads to structure factors which deviate from experimental data only half as much as previously reported LDA results. The improvement comes mainly from the description of the core charge density. The GGA of Engel and Vosko is even better for the core electrons, but the valence electrons are not described as well. The experimental and theoretical description of the covalent bonding in silicon is studied by means of difference maps and multipole expansions. The limitation of the multipole model is investigated by fitting both experimental and theoretical charge densities.

1. Introduction

Accurately measured structure factors of silicon provide an excellent test for the charge densities calculated from various solid-state theories. The de facto standard test of theoretical approximations is based either on single-particle energies (comparing e.g. ionization potentials or band gaps) or on quantities derived from the total energy, like equilibrium lattice constants and bulk moduli. In the former case, excited states are involved, and thus density functional theory (DFT), which is designed for ground-state properties, cannot be applied rigorously. This is in contrast to the latter case, namely a comparison of structural parameters, a standard test for theory, which does not, however, offer significant insight into chemical bonding. On the other hand, the crystal charge density is a ground-state property and is the key quantity in DFT. It is quite sensitive to the crystal potential and provides valuable three-dimensional information. The main limitation in using the charge density is its availability. While energy levels and structural properties can be measured very precisely, the charge density is generally less accurately known. An exception is the case of silicon, since large, perfect single crystals can be grown and the highly accurate x-ray pendellösung technique can be applied [1]. Unfortunately, for other materials, such

§ Author to whom any correspondence should be addressed; e-mail: zuo@phyast.la.asu.edu.

0953-8984/97/367541+21$19.50

accurate structure factors are rarely available. However, the recent development in electron diffraction methods promises to change this picture [2].

Compared to the experimental measurement of charge densities, their theoretical computation is relatively straightforward due to the advances in solid-state theory and the availability of highly sophisticated algorithms, such as the full-potential linearized-augmented-plane-wave (LAPW) and the linear-combination-of-atomic-orbitals Hartree–Fock (LCAO-HF) methods. In the case of silicon, the best agreement between theory and experiment previously reported gave an R-factor of 0.21% [3]. This is a low value compared with the often significantly larger R-factor for different x-ray measurements based on the kinematical approximation. The largest effect of charge redistribution due to chemical bonding in silicon is on the low-order reflections with s ($\equiv(\sin\theta)/\lambda$) smaller than 0.4 Å^{-1}. The extinction effect in these low-order reflections is usually large, and is the main factor limiting the accuracy of kinematical methods. For the high-order reflections, the difference between the structure factors of the real crystal and a superposition of neutral spherical atoms is usually small. In the case of Si, this difference is less than 0.01×10^{-3} electrons/atom for $s > 0.6$ Å^{-1}. For this reason most experimental measurements of charge distributions usually involve a limited number of low-order reflections.

For the charge density of silicon, experimental structure factors for up to reflection (880) are available from five independent measurements by Aldred and Hart [1], Teworte and Bonse [4] and Saka and Kato [5] made using the x-ray single-crystal pendellösung method. Additional measurements for specific reflections were also made by means of electron diffraction [6, 7]. The consolidation of x-ray data sets by Cumming and Hart [8] shows an averaged accuracy of $3–5 \times 10^{-3}$ electrons/atom. The theoretical charge density of silicon has also been calculated by a number of methods (for a selective listing see [9]). An early comparison of the experimental and theoretical results was made by Spackman [10]. Since then, the agreement between theory and experiment has been substantially improved with the more recent calculations of [3, 9] using the LAPW method which are based on DFT and the LCAO-HF method [11], respectively. The LAPW calculations of [3] used the local density approximation (LDA) for the exchange and correlation potential. The residual difference between the theoretical structure factors of [3] and experiment is still large compared to the estimated experimental accuracy. This difference is systematic rather than random and is as large as 20×10^{-3} electrons, about ten times the estimated experimental accuracy. The largest differences occur for reflections from (311) to (440), with the exception of (222), and are all negative. This suggests a significant deviation between the experimental and calculated charge density in the core region up to around 0.6 Å from the nucleus. The Hartree–Fock LCAO study made by Pisani *et al* [11] using the CRYSTAL program is in better agreement with experiment for the high-order reflections. However, their low-order structure factors obtained with an optimized basis set (corresponding to the lowest total energy) differ significantly from experiment.

Theoretically, there are two fundamentally different ways to treat exchange and correlation effects: one is based on the Hartree–Fock (HF) approximation and the other uses density functional theory (DFT). In the HF method, exchange is given exactly, while correlation effects are (by definition) completely neglected but can be incorporated by means of elaborate techniques such as the configuration interaction method. In DFT both exchange and correlation effects are included, but in practice only approximately. The simplest version is based on the homogeneous electron gas and leads to the LDA. If not only the density $\rho(r)$ at a given point r, but in addition also its gradient, are used to determine exchange and correlation, then a generalized gradient approximation (GGA) can be formulated which satisfies various physical constraints. Among the various forms of GGA which have been

proposed, the functional of Perdew and Wang (PW91) [12] is the most commonly used and tested. It is constructed by means of a real-space cut-off of the spurious long-range part of the density gradient expansion for the exchange–correlation hole surrounding an electron. It gives a good description of the atomic energy, largely due to a cancellation of local errors [14], but the corresponding exchange–correlation potential is a derived quantity which does not agree too well with the exact potential. Improvements of the cohesive energy of solids have been reported for PW91-GGA calculations [12, 13], but in some cases, where the LDA already gives good lattice constants and bulk moduli, the GGA tends to overcorrect the LDA results [13]. Engel and Vosko (EV) [14] proposed a different GGA functional based on the virial relation for the exchange energy, which is intended to reduce the local error in the exchange potential. However, it has been found that the EV total energies are poor, which leads to large discrepancies with experimental structural parameters (see e.g. Dufek *et al* [38]). Both versions of the GGA, PW91 and EV, are tested in this paper. The systematic differences between the LDA results of [3] and experiment for the high-order reflections are probably due to the inadequate treatment of core electrons within the LDA. To test the effect of improved exchange and correlation potentials on the charge density, we will study the charge density using the GGA.

In studying crystal bonding, the charge-density difference between the crystal and an atomic reference is often used. For theoretical studies, it is natural to use an atomic reference calculated with the same approximation as for the solid. However, for experimental studies, the choices are not so clear. Commonly used atomic charge densities in diffraction studies are the relativistic Hartree–Fock calculations of Doyle and Turner listed in the *International Tables for Crystallography* [15] and the parametrized non-relativistic Hartree–Fock calculations of Clementi and Roetti [16]. These are single-configurational calculations, which ignore electron correlation. More recently, there have been new calculations of atomic charge densities including different approximations for correlation effects. Rez and Rez [17] used the multi-configurational Dirac–Fock (MCDF) method of Grant *et al* [18] for the entire periodic table. A more limited calculation for the elements from He to Ar was carried out by Wang *et al* [19] again using the MCDF method, but without the extended average-level model [18] applied in [17]. Meyer *et al* [20] reported atomic scattering factors using a multi-reference singly and doubly excited configuration interaction method. Here, we will compare various atomic charge densities for silicon. The core electron density will be tested against the experimental high-order structure factors of silicon, where the contribution of valence electrons is negligible.

In this paper, we will also compare the theoretical and experimental crystal charge densities by model fitting. One of the important questions about the crystal bonding is that of whether an atom expands or contracts in the crystal environment. Recent measurements of the silicon mean potential report a substantially lower value than for a neutral spherical atom [21], which suggests an overall contraction of the Si atom in the crystal [22]. This is in contrast to the results of a multipole analysis, which gives a $\sim$6% valence expansion [1] and a 0.5% L-shell expansion [23]. The result of a multipole analysis hinges on the validity of the model, especially the significance of individual parameters in the fitting model. By applying the model analysis to both experimental and theoretical structure factors, the validity of the multipole model will be studied.

2. Experimental structure factors of Si

The room temperature experimental structure factors of silicon used here are taken from the consolidated set of Cumming and Hart (CH) [8] and the Saka and Kato (SK) [5] set.

Table 1. Room temperature experimental and theoretical form factors of silicon in units of number of electrons per atom. The experimental data, which were corrected for the anomalous absorption and nuclear scattering, are taken from Cumming and Hart [8] and Saka and Kato [5] with those from [5] marked with asterisks. The estimated errors (given in parentheses) for the data set of [8] are taken from reference [25]. The theoretical scattering factor is multiplied by the temperature factor $\exp(-0.4668g^2/4)$.

(h, k, l)	Experiment	MCDF[a]	MCDF-WBSJ[b]	CI[c]	LAPW-LDA[d]	LAPW-GGA[e]	LAPW-GGA(EV)[f]	HF-LCAO[g]
111	10.6025(29)	10.4160	10.4273	10.4391	10.5995	10.6065	10.6605	10.598
220	8.3881(22)	8.4432	8.4423	8.4497	8.3952	8.3929	8.3752	8.3902
311	7.6814(19)	7.8216	7.8198	7.8203	7.6909	7.6897	7.6670	7.6813
222	0.182(1)	0.0000	0.0000	0.0000	0.161 47	0.166 43	0.180 88	0.187 86
400	6.9958(12)	7.0532	7.0522	7.0460	6.9933	7.0007	7.0025	7.0042
331	6.7264(20)	6.6692	6.6687	6.6611	6.7031	6.7149	6.7221	6.7370
422	6.1123(22)	6.1015	6.1016	6.0938	6.0897	6.1028	6.1146	6.1130
333	5.7806(21)	5.7935	5.7939	5.7858	5.7552	5.7688	5.7845	5.7632
511	5.7906(27)	5.7935	5.7939	5.7858	5.7761	5.7895	5.8044	5.8018
440	5.3324(20)	5.3244	5.3249	5.3182	5.3136	5.3270	5.3377	5.3375
531*	5.0655(17)	5.0664	5.0670	5.0607	5.0490	5.0621	5.0731	
620*	4.6707(9)	4.6713	4.6720	4.6659	4.6561	4.6685	4.6786	
533*	4.4552(11)	4.4535	4.4542	4.4487	4.4444	4.4558	4.4649	
444	4.1239(18)	4.1194	4.1200	4.1165	4.1085	4.1192	4.1268	4.1210
711*	3.9282(22)	3.9349	3.9355	3.9328	3.9229	3.9331	3.9381	
551	3.9349(34)	3.9349	3.9355	3.9328	3.9248	3.9348	3.9403	3.9359
642	3.6558(54)	3.6516	3.6522	3.6499	3.6427	3.6519	3.6561	3.6513
731*	3.4919(11)	3.4949	3.4955	3.4933	3.4869	3.4956	3.4992	
553*	3.5055(14)	3.4949	3.4955	3.4933	3.4883	3.4972	3.5011	
800	3.2485(34)	3.2540	3.2545	3.2526	3.2470	3.2549	3.2563	3.2518
733*	3.1270(14)	3.1204	3.1210	3.1193	3.1154	3.1229	3.1239	
822*	2.9111(15)	2.9145	2.9150	2.9139	2.9105	2.9172	2.9173	
660	2.9143(16)	2.9145	2.9150	2.9139	2.9105	2.9172	2.9174	2.9121
555	2.8009(21)	2.8002	2.8007	2.7999	2.7947	2.8009	2.7998	2.7945
751*	2.8006(25)	2.8002	2.8007	2.7999	2.7976	2.8039	2.8037	
840*	2.6200(7)	2.6236	2.6240	2.6239	2.6219	2.6276	2.6266	
911*	2.5325(8)	2.5253	2.5257	2.5259	2.5242	2.5296	2.5279	
753*	2.5274(29)	2.5253	2.5257	2.5259	2.5229	2.5282	2.5264	
664*	2.3677(9)	2.3731	2.3735	2.3742	2.3733	2.3781	2.3760	
844	2.1506(24)	2.1564	2.1568	2.1580	2.1581	2.1622	2.1597	2.1531
880	1.5325(26)	1.5317	1.5319	1.5340	1.5370	1.5390	1.5360	1.5289

[a] Calculated with the atomic charge density of [17]; for details, see the text.
[b] Calculated with the atomic scattering factors listed in [19].
[c] Calculated with the atomic scattering factors listed in [20].
[d] The crystal scattering factor calculated with the LAPW and the LDA for exchange and correlation.
[e] The crystal scattering factor calculated with the LAPW and the PW91-GGA [12].
[f] The crystal scattering factor calculated with the LAPW and the GGA of Engel and Vosko [14].
[g] Taken from reference [11]; obtained using Hartree–Fock LCAO method.

The CH data set is less complete than the SK set. The CH data set is the average of the experimental measurements by Aldred and Hart [1] and Teworte and Bonse [4] with Ag Kα_1 and Mo Kα_1 wavelengths plus the measurements of Saka and Kato [5]. For monatomic Si crystal, it is convenient to discuss the form factor of Si, which is related to the structure factor by

$$f(h,k,l) = F(h,k,l) \Big/ 8\cos\left(\frac{\pi}{4}(h+k+l)\right). \tag{1}$$

For (222), $f(h,k,l) = F(h,k,l)/4$. Table 1 lists both the experimental form factors $f(h,k,l)$ and their estimated errors, with those from the SK data set marked with asterisks. $f(222)$ is taken from the measurement of Alkire, Yelon and Schneider [24]. The estimated error for the data set of CH is taken from reference [23], which is the average of the estimated errors given by [1] and [4]. The estimated error of [23] is somewhat smaller than the actual fluctuations from the mean found in the five measurements; for example in the case of (111), the averaged standard error from the five measurements is about 5.1×10^{-3} electrons/atom and the estimated error given by [23] is 2.9×10^{-3} electrons. Among the five experimental data sets, the Saka and Kato measurements appear to be the best, giving the lowest standard deviation (average about 3.6×10^{-3} electrons) from the averaged structure factors of CH [8]. For the low-order structure factors, such as (111), the estimated accuracy reported by Saka and Kato [5] is significantly higher than those from other measurements. The experimental x-ray structure factors were corrected for anomalous dispersion and nuclear scattering [8]. The anomalous dispersion was taken from the measurements of Deutsch and Hart [25]. In table 1, the corrected structure factors of the SK data set are taken from table 2 of Lu and Zunger [3]. Structure factors of silicon have also been measured by means of electron diffraction [7, 6], for which, in contrast to the case for x-ray diffraction, anomalous dispersion is small and negligible. The electron diffraction measurement of [7] gives $f(111) = 10.613(7)$ and $f(222) = 0.186(4)$, in good agreement with the x-ray measurements. In particular, the electron diffraction measurement of (222) includes both amplitude and phase [26], while the measurement of Alkire *et al* [24] is for the amplitude only. The agreement between electron and x-ray results independently confirms the anomalous dispersion correction used by [8].

The charge density of real crystals is affected by both chemical bonding and thermal vibrations. In the adiabatic harmonic approximations for thermal vibrations, the measured silicon crystal charge density is simply the convolution of the static charge density and the temperature factor:

$$F(h,k,l) = F^s(h,k,l)\exp[-B(h^2+k^2+l^2)/4a^2]. \tag{2}$$

Here $F^s(h,k,l)$ is the static structure factor. The temperature factor is a Gaussian function with the Debye–Waller factor B as a parameter, which describes the temperature effect due to atomic motions on the charge density. The separation of the crystal charge density into a static atomic density and a temperature factor is conceptual in this case; it does not affect the structure factor formula of equation (2) as long as we assume the same thermal vibrations for all electrons. The contribution of anharmonic thermal vibrations to the structure factor has been obtained by Batterman and co-workers [39] by measuring the temperature dependence of forbidden reflection intensities with both x-ray and neutron diffraction. The reported anharmonic force constant β ranges from 1.38 to 3.38 eV Å^{-3}, assuming an isolated-atom model of thermal vibrations [27]. However, there is little evidence for such a large upper limit of β from the structure factors measured at room temperature. Refinements by Deutsch

[23] indicate an upper limit of 0.8 eV Å^{-3} for β. In view of this controversy, the effect of anharmonic thermal vibration will be ignored in the initial analysis and further discussed in section 7.

3. Theoretical structure factors of Si

Several theoretical structure factors are included in this study. Our LAPW calculations of the crystal charge density were carried out with both the LDA and the GGA. The LAPW program used here is the *WIEN 95* package written by Blaha, Schwarz, Dufek and Augustyn of the Technical University of Vienna [28, 29]. For the LDA functional the Perdew and Wang parametrization of the Ceperley and Alder results [30] is used, while for the GGA both the functional PW91 [12] and that of Engel and Vosko [14] are employed. Our LAPW method treats core and valence electrons equally, and the charge densities are obtained self-consistently. The parameters involved in the calculation are numerical in nature, controlling the convergence of the calculations. We have used 72 k-points in the irreducible Brillouin zone, a maximum angular momentum for the radial wave functions $l_{max} = 10$, a muffin-tin radius 1.8 au, 381 (661 for the GGA) logarithmic radial mesh points inside the atomic spheres and a plane-wave cut-off of $R_{MT}K_{max} = 8$ or 9. Both the muffin-tin radius and the number of k-points are varied to ensure convergence. The structure factors calculated using the LDA agree with the results published by Lu and Zunger [3] to better than 2×10^{-3} electrons/atom. For the GGA, 661 radial mesh points up to the muffin-tin radius was found to be sufficient. The structure factors are calculated by means of a Fourier transformation of the LAPW charge density [28, 29].

We also compare here the published structure factors of the HF-LCAO calculations by Pisani, Dovesi and Orlando [11], who included the reflections of the data set from [8]. This provides a comparison between HF and LDA results for crystals. Here we use the data set marked in their study as 8-41G**, although their 8-41G* set agrees better with the experimental structure factors. The difference between these two is that in 8-41G* the outer exponent of the sp-Gaussian-type orbital (GTO) is fixed, while in 8-41G** it is variationally optimized, resulting in a less diffuse outer sp GTO and also in a lower total energy. Originally, Pisani *et al* [11] compared their results with the experimental structure factors listed by Spackman [10] rather than the consolidated data of [8], but later a comparison with the 8-41G** results was made in [9].

Structure factors simply calculated according to a superposition of neutral atomic densities are also included in this study. The atomic scattering factors are obtained from two different approaches; one is based on Hartree–Fock (HF) or Dirac–Fock (DF) theory in the relativistic case, and the other is based on DFT (the Hartree–Fock–Slater (HFS) or Dirac–Slater (DS) theory in the relativistic case). The DF atomic scattering factors are obtained from the charge density of [17], where the multi-configurational Dirac–Fock (MCDF) program of Grant *et al* [18] was used. The DS calculations are done with a modified program written by Desclaux [31], which is part of the *WIEN 95* package [28]. In both cases, atomic scattering factors are obtained by numerical integration with a three-point Simpson rule on a logarithmic radial mesh. The atomic scattering factors of MCDF theory are slightly different from those originally published by [17], probably due to the difference in the numerical integration. A number of published atomic charge densities for silicon are also included here for comparison. The atomic scattering factors of Clementi and Roetti [16] have been obtained using the non-relativistic Hartree–Fock–Roothaan method. The Clementi and Roetti atoms are popular in x-ray diffraction due to the Slater orbital form of the parametrization. Fourier transformation of the Slater orbitals is carried out

with a program provided by O'Keeffe [32]. We have also included the recently published atomic scattering factors of [19] and [20], which were obtained using MCDF theory and the multi-reference singly and doubly excited configuration interaction method, respectively. They are included to show the effects of electron correlation on atomic charge densities. The relativistic HF scattering factors of Doyle and Turner from the *International Tables for Crystallography* [15] are also compared here.

All of the theoretical structure factors are calculated with a lattice constant of $a = 5.4307$ Å [33], with the exception of the HF-LCAO results [11], which use $a = 5.431$ Å. To compare with experiment, all of the theoretical structure factors are multiplied by a temperature factor of $\exp(-Bg^2/4)$ with $B = 0.4668$ Å^2 described in the next section.

Table 2. A comparison between the experimental and theoretical form factors for (440) and higher with the Debye–Waller factor as a free parameter. The R-factor and GOF are defined as follows: $R = \sum |f^{\text{theory}} - f^{\text{exp}}|/|f^{\text{exp}}|$; $\text{GOF} = (1/N)\sum_{i=1}^{N}(1/\sigma_i^2)(f_i^{\text{theory}} - f_i^{\text{exp}})^2$. The GOF is calculated with the average variance of 0.0022^2. For details, see the text. For the abbreviations not given in the footnotes, see table 1.

	B (Å^2)	R-factor (%)	GOF
HFR[a]	0.4628	0.114	4.8
RHF[b]	0.4668	0.112	4.6
MCDF	0.4668(6)	0.111	4.5
MCDF-WSBJ	0.4671	0.112	4.6
CI (MR-SD)	0.4667	0.145	7.2
DS-LDA[c]	0.4635	0.28	31
DS-GGA[d]	0.4670	0.21	17
DS-GGA(EV)[e]	0.4669	0.14	6.8
LAPW-LDA	0.4652	0.21	15
LAPW-GGA	0.4687	0.14	6.2
LAPW-GGA(EV)	0.4689	0.118	4.4
LCAO-HF[f]	0.4654(7)	0.105	3.6

[a] Calculated with the atomic charge density of reference [16].
[b] Calculated with the atomic scattering factors listed in reference [15].
[c] The atomic scattering factor obtained using the Dirac–Slater method and the LDA.
[d] The atomic scattering factor obtained using the Dirac–Slater method and the PW91-GGA.
[e] The atomic scattering factor obtained using the Dirac–Slater method and the GGA of Engel and Vosko.
[f] Evaluated with the data set of [8] and nine reflections.

4. Comparison of the experimental and theoretical structure factors

Table 1 lists selected experimental and theoretical form factors at room temperature. For low indices there are obvious differences between the experimental structure factors and atomic structure factors, especially for (111), because the crystal bonding is neglected. However, this difference diminishes as g increases. Figure 1 plots the shell-by-shell contributions to the atomic scattering (form) factor obtained using the MCDF method, from which we can see the well known feature that the high-order structure factors are dominated by the core electrons, especially the 1s electrons. Thus the accurately measured high-order structure factors can be used to test the core part of the atomic calculations. Table 2 shows a comparison between theory and experiment based on 22 form factors for the reflections from (440) to (880) using the goodness-of-fit (GOF) and R-factor criteria. In this comparison the Debye–Waller factor B is treated as an adjustable parameter. The

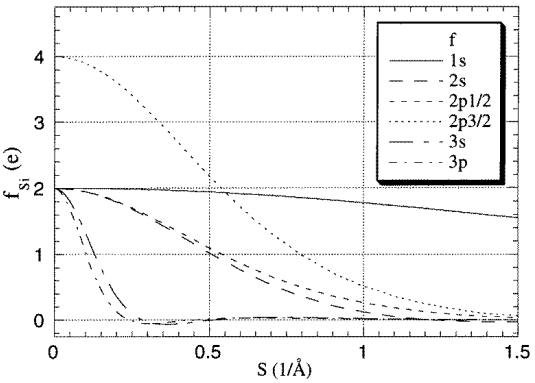

Figure 1. Shell-by-shell contributions to the atomic scattering factor of Si calculated by the MCDF method.

GOF is evaluated with a mean estimated variance of $\sigma^2 = 0.0022^2$. This mean variance is used because of the concern about the reliability of the estimated accuracy of each reflection, especially for the SK data set [5]. The best agreement with the high-order reflections is obtained with the HF-LCAO calculations of Pisani *et al* [11], for which the comparison was made with the nine available reflections ((440) and higher). Among the atomic models, both the R-factor and GOF criteria indicate that correlated Hartree–Fock models are better than approaches based on DFT. Specifically, the atomic scattering factors of MCDF calculations yield the best results with an R-factor of 0.11%, a GOF of 4.5 and a Debye–Waller factor of $B = 0.4668$ Å^2. Among the atomic charge densities calculated using the Dirac–Slater method, the GGA of Engel and Vosko gives the best description of the high-order structure factors. Its R-factor of 0.14% is significantly lower than those of the PW91-GGA and the LDA. Using the same approximation for the exchange and correlation, the LAPW crystal calculation is always better than the atomic one. Presumably, this is due to the small but non-negligible crystal bonding effects for these high-order reflections. The same can be said to the improvement of the crystalline HF-LCAO results over similar atomic calculations [16]. The LAPW calculation with the GGA gives a factor-of-two improvement over the LDA. The GOF of 4.5 obtained with the MCDF atomic scattering factor suggests that not all of the information in the experimental data is exhausted. Possible improvements can come from a better description of crystal bonding and anharmonic effects. For the high-order reflections, the atomic scattering factors obtained with the RHF (Doyle and Turner [15]) and MCDF [17, 19] methods are very similar, with almost the same R-factor and Debye–Waller factor. The Clementi and Roetti atomic structure factors give a significantly smaller Debye–Waller factor than the RHF or MCDF methods. The difference is probably due to the neglect of relativistic effects in the HF method used in [16], which results in slightly lower contributions to the high-angle scattering factors. Also the recently published (non-relativistic) atomic scattering factors obtained by Meyer *et al* [20] using multi-reference singly and doubly excited configuration interaction do not improve upon the Dirac–Fock results and have a significantly higher R-factor and GOF. This analysis indicates that for the core electrons relativistic effects are more important than correlation.

Figure 2 plots the difference between radial charge densities $r^2\rho(r)$ obtained with the MCDF method and the GGAs and LDA. Figure 2(a) shows the charge-density difference between LDA and MCDF for each orbital, while figures 2(b) and 2(c) show

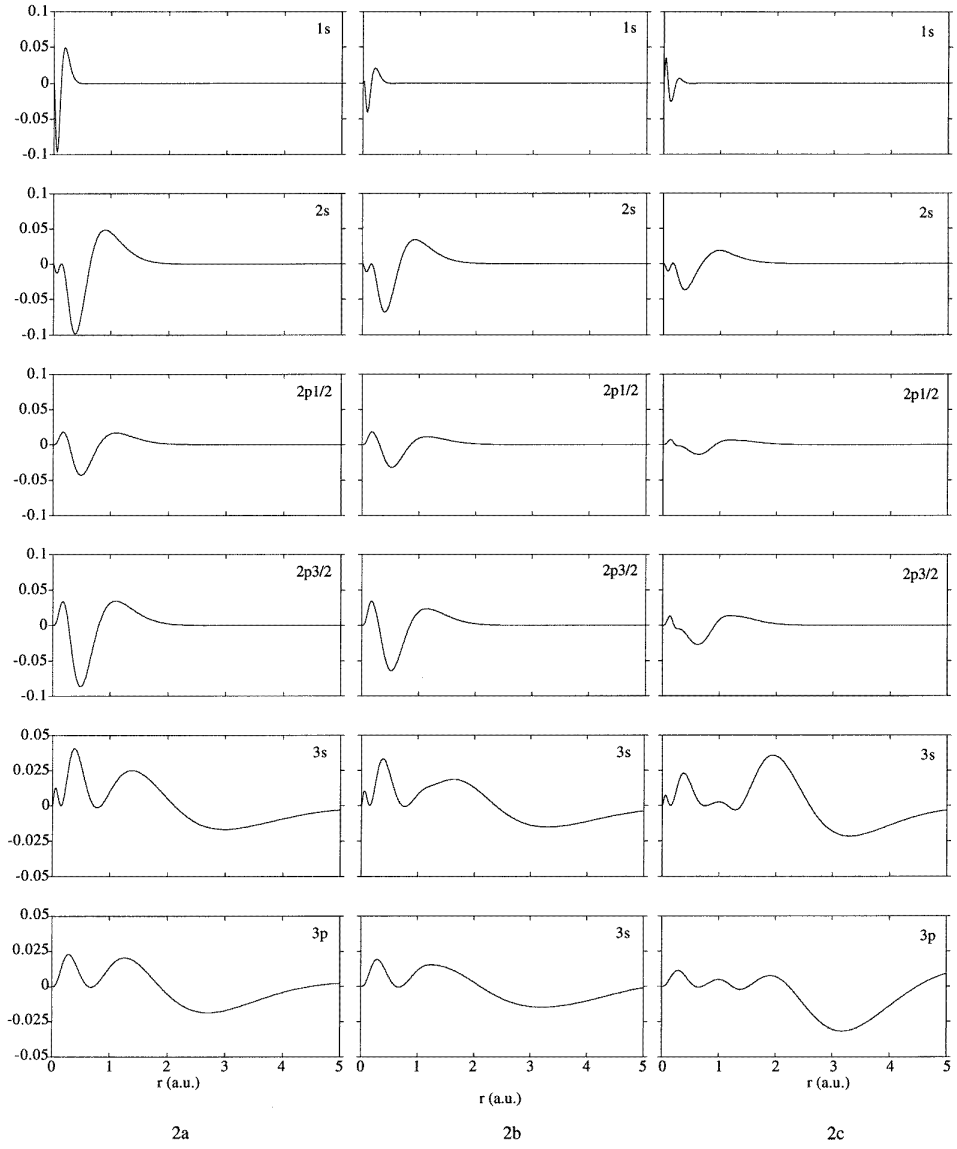

Figure 2. The shell-by-shell charge density $r^2\rho(r)$ difference between the DS atom using GGAs or the LDA and the MCDF atom; (a) LDA, (b) the PW91-GGA and (c) the GGA of Engel and Vosko. For details see the text.

the corresponding difference for the of PW91-GGA and the EV-GGA, respectively. The curves in all three parts of the figure are quite similar in their overall shape. However, the differences from the 'exact' densities obtained using PW91 (figure 2(b)) are already smaller than for the LDA (figure 2(a)). The EV-GGA further improves the core electron density, especially for the 2s and 2p electrons, for which the improvement of the PW91-GGA over the LDA is small. On the other hand, the valence 3s and 3p densities are worse with the EV-GGA. This visually demonstrates that the improvement in the agreement with the high-

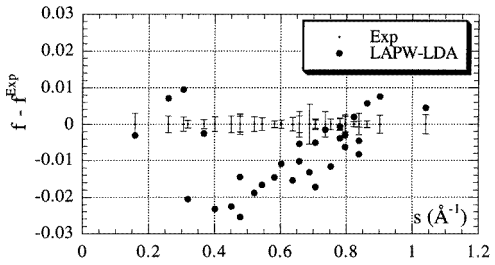

(a)

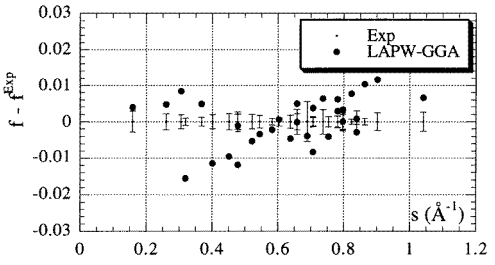

(b)

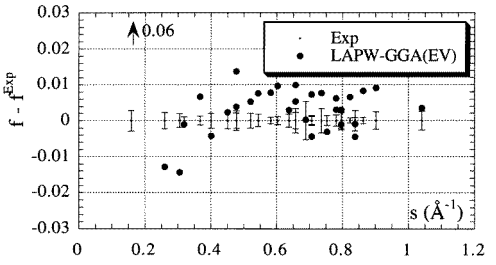

(c)

Figure 3. The form factor difference between theory and experiment for: (a) the LAPW using the LDA; (b) the LAPW method using the PW91-GGA; (c) the LAPW method using the GGA of Engel and Vosko; (d) the HF LCAO method of reference [11], where 1 and 2 denote the basis sets 8-41G* and 8-41G** respectively; and (e) the atomic MCDF model. The form factor is in units of number of electrons per atom.

order experimental structure factors for the GGA comes from a better core charge density, and that the EV-GGA is superior to the PW91-GGA in the core region, but worse even than the LDA in the valence region.

In table 3 the crystal form factors calculated with the LAPW method using the LDA and both GGAs and the published HF-LCAO results are compared with all 31 experimental structure factors using the temperature factor of $B = 0.4668$ obtained above. The residual difference between theory and experiment is plotted in figure 3. The best overall agreement is obtained with the LAPW method using the PW91-GGA, and its lowest R-factor is almost a factor-of-two improvement over the LDA. The slightly worse R-factor and large GOF for the EV-GGA is mainly due to the (111) structure factor, which is significantly larger than that from experiment. Figure 3 also shows that the difference between experiment and the LAPW method using the LDA or PW91 is systematic. Both PW91 and the LDA consistently

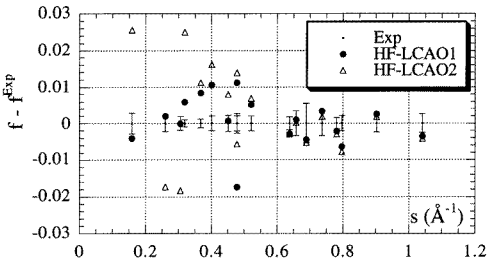

(d)

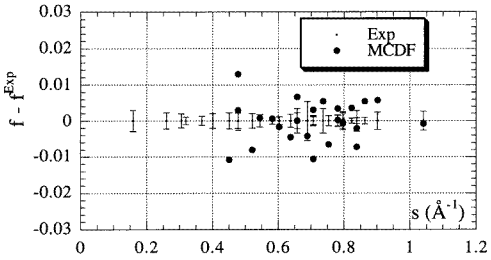

(e)

Figure 3. (Continued)

Table 3. A comparison between the experimental and selected theoretical form factors of table 1 with all structure factors included.

	LAPW-LDA	LAPW-GGA (PW91)	LAPW-GGA (EV)	LCAO-HF*	MCDF
R-factor	0.24%	0.13%	0.18%	0.20%	0.60%
GOF	30	8.8	32	31	632

* Evaluated with data set 1 and 18 reflections.

underestimate the scattering factor in the *s*-range of about 0.4 to 0.8 Å^{-1} and overestimate it from 0.8 to 1.1 Å^{-1}. The improvement of the *R*-factor with PW91 is largely due to the improved description of core electrons as compared to that of the LDA (see above). Such a systematic trend is almost absent for the GGA of Engel and Vosko.

5. The charge density of silicon

The theoretical static charge density of silicon can be computed with high precision subject to a well chosen basis set, and a good description of exchange and correlation as well as relativistic effects. Determination of an experimental charge-density map by Fourier synthesis using measured structure factors is difficult due to the limited number of structure factors and their restricted accuracy. However, a comparison between theory and experiment can still be made based on (1) a truncated Fourier series map of limited resolution and (2) model fitting with the same limitations on theory and experiment. The truncated Fourier series limits the resolution of the synthesized map; finite fluctuations can also be introduced from the sharp cut-off. Fluctuations in the deformation map (defined as the difference between the crystal and superimposed spherical atomic charge densities) are smaller due to

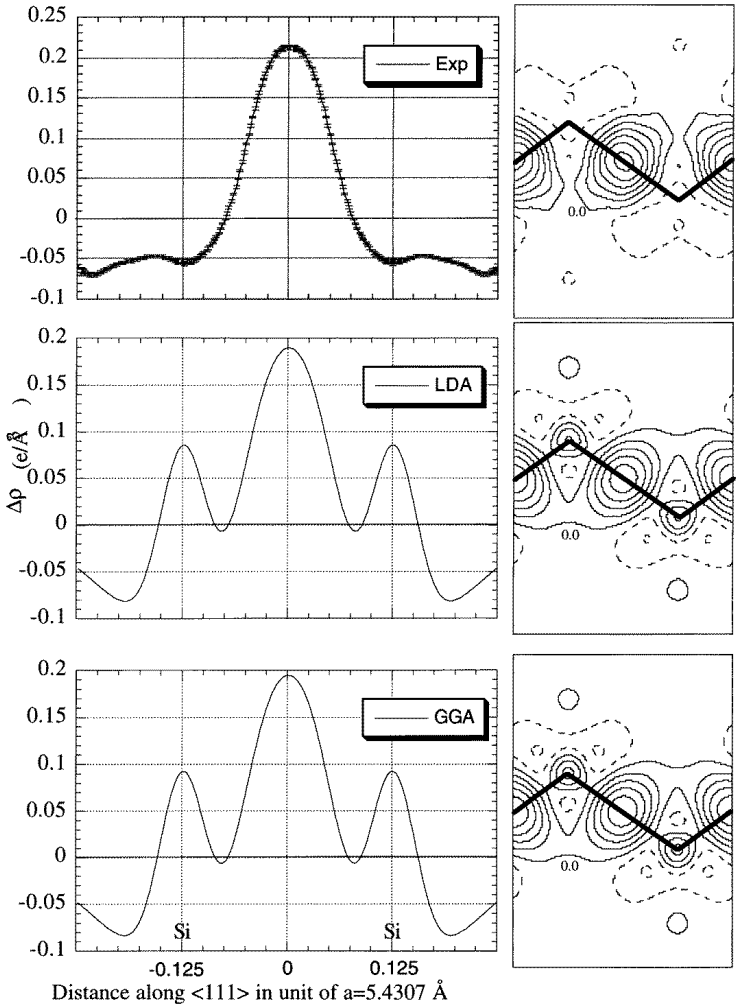

Figure 4. A deformation map and a profile along [111] of the Si crystal charge density synthesized with the 31 independent reflections of table 1. The contour map is plotted with a increment of 0.04 e Å^{-3} and dashed lines show the charge deficiency. The zero contour level is marked in each panel. Top panels: experiment; middle panels: the LAPW method using the LDA; and bottom panel: the LAPW using the PW91-GGA. The profile is taken through the Si–Si bond. The black lines connect the Si atoms.

the rapidly decreasing difference between the crystal and atomic high-order structure factors. The limited resolution does not affect the slowly varying charge density between the silicon atoms much, whereas it does preclude any quantitative comparison of the rapidly varying charge density in the atomic core region (see below). Figure 4 shows the synthesized deformation maps obtained using the limited reflections of table 1. The experimental deformation map uses the MCDF atom as a reference, while DS atoms with the LDA or PW91-GGA are used for the corresponding LAPW deformation map. The error bars shown in the top panel of figure 4 were calculated according to Maslen [34]. The LDA and the PW91-GGA maps both reproduce well the bonding charge-density peak in the

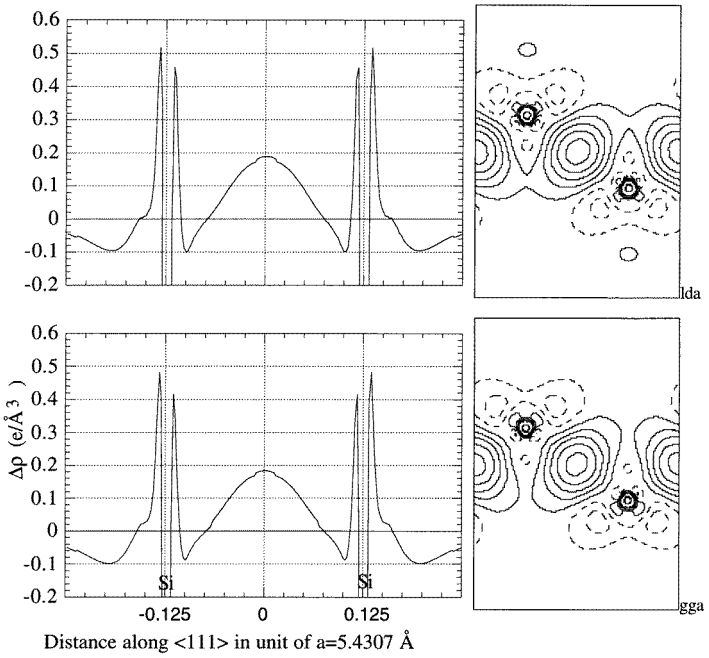

Figure 5. A high-resolution deformation map synthesized directly from the LAPW basis function for (top panels) the LDA and (bottom panels) the PW91-GGA. The contour map is plotted with an increment of 0.04 e Å^{-3} and dashed lines show charge deficiency.

silicon–silicon bond, with peak values of 0.189 and 0.194 e Å^{-3}, respectively, compared to the experimental values of 0.213 ± 0.003 e Å^{-3}. The largest difference between the experimental and theoretical deformation maps of figure 4 is that both the LDA and the GGA predict a significant 'charge pile-up' at the atomic site, while the experimental map shows a relatively flat negative distribution. A high-resolution deformation map synthesized directly from the LAPW basis function is shown in the top and bottom panels of figure 5 for the LDA and PW91-GGA. The charge 'pile-up' observed in figure 4 at the atomic site is actually due to a strong nodal-type charge-density modulation in the atomic core region, which is strongly negative at the nucleus and positive in the immediate surrounding area.

The variance at a point in the difference charge-density map is calculated according to (reference [34])

$$\sigma^2(\Delta\rho) = \sum_i \left[2V^{-1} \sum_e \cos(2\pi \boldsymbol{s}_{ie} \cdot \boldsymbol{r}) \right]^2 \sigma^2(\boldsymbol{s}) \tag{3}$$

where the i and e denote the independent and symmetry-related reflections, respectively. The top panel of figure 4 shows the standard deviation estimated from equation (3). The interpretation of σ is difficult because of the correlation between different points in the difference map arising as the result of the Fourier transformation. For details about the significance of σ, see [34]. Alternatively, the reliability of a particular feature of finite size in the charge-density difference can be determined by applying the standard statistical test using

$$\chi^2 = \sum_s \sigma^{-2}(s)[\Delta F(s)]^2 / v \tag{4}$$

where ΔF is the contribution to the structure factor from the tested part of the difference map and v is the number of reflections included in the evaluation. To test whether the oscillations near the core are detectable experimentally, we isolate the oscillating feature in the theoretical LAPW difference map by its outside zero boundary, neglect the small non-spherical distortion, and evaluate its contribution to the structure factor by Fourier transformation. The results are shown in figure 6. Overall, the resulting change in the structure factor is very small, less than 5×10^{-3} electrons/atom in the range of measurable s-values. Applying equation (4) and using the estimated accuracies listed in table 1, we obtain a χ^2-value of 0.64. This suggests that with the current experimental precision it is not possible to experimentally verify the existence of the oscillating charge density in the core region observed in the LAPW difference map.

Table 4. The scaling of the theoretical LAPW core charge density.

	1s	2s	$2p_{1/2}$	$2p_{3/2}$
GGA (PW91)	1	0.999 58	0.999 24	0.999 25
LDA	1	0.9995	0.999 11	0.999 09

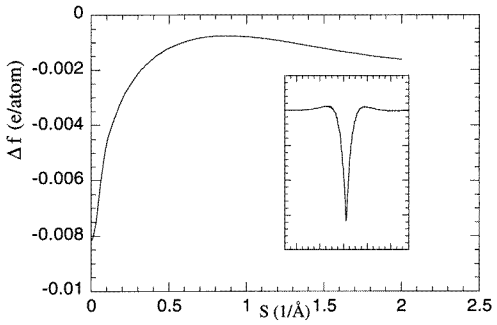

Figure 6. Contributions of the core-region (within a 0.2 Å radius from the Si nucleus) nodal-type charge modulation in the LAPW difference map to the atomic scattering factor. For details, see the text.

The silicon 1s2s2p core electrons are considered to be localized, since there is very little overlap between these core electrons at different sites. Thus the effect on the core electrons of forming a crystal can be directly studied in the theoretical charge density by comparing with the respective atomic densities without the usual ambiguity associated with separating crystal charge densities into atomic contributions. In a previous study, Deutsch [23] reported a 0.5% L-shell expansion from his multipole model refinement of experimental structure factors of the CH data set. Figure 7 plots the difference between the radial charge density $r^2\rho$ of the crystal and atomic core electrons from the LAPW calculations, which indicates that the core electrons expand slightly in the crystal. A direct fitting to each core orbital shows that the difference between crystal and atomic core electrons can be well described by scaling. The results are shown in table 4. In both cases, GGA and LDA, the 1s electron remains virtually unchanged by bonding. The electrons in the L shell expand slightly by 0.09% to 0.04%; this is five to ten times smaller than the expansion estimated by Deutsch [23]. Figure 7 also shows that the charge-density difference due to the core electrons is relatively small compared to the charge difference seen in figure 5. This suggests that the

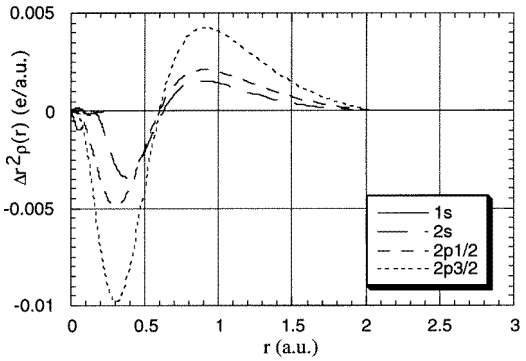

Figure 7. The difference between the radial charge density $r^2\rho(r)$ of the Si core electrons in the crystal environment (calculated by means of the LAPW method) and in a free atom.

large fluctuations of figure 5 in the core region are largely due to the valence electrons. A similar conclusion was reached in [3].

6. Multipole model refinement

In the multipole model given by Dawson [35], Stewart [36] and Coppens *et al* [37], the structure factor of silicon is expanded in terms of the Kubic harmonics:

$$F(h,k,l) \approx 8\cos\phi\{f_c + \delta_{c,4} - f_{a,3}\tan\phi\}\exp(-Bs^2) \tag{5}$$

with non-spherical terms in the charge density up to fourth order. The 'atomic' scattering factors $F(h,k,l)/8\cos\phi$ are listed in table 1. Here the phase $\phi = (h+k+l)\pi/4$. The f_c, $\delta_{c,4}$, and $f_{a,3}$ are the spherical, fourth- and third-order Kubic harmonic parts of the generalized 'atomic' scattering factor of silicon, respectively. Again, harmonic thermal vibration is assumed. The spherical term f_c is taken as the sum of suitable scaled atomic orbital scattering factors:

$$f_c(\boldsymbol{s}) = \sum_{nl} f_{nl}(\boldsymbol{s}/\kappa_{nl}) \tag{6}$$

where nl designates the shell and κ_{nl} is a scaling constant for each shell, which is usually taken as one except for the valence shell. The non-spherical third- and fourth-order terms are expressed by

$$f_{a,3} = O\frac{8\pi\alpha^7}{6!}\frac{hkl}{(h^2+k^2+l^2)^{3/2}}\int_0^\infty r^4\exp(-\alpha r)\,j_3(4\pi sr)\;\mathrm{d}r \tag{7}$$

$$\delta_{c,4} = H\frac{8\pi\alpha^7}{6!}\frac{640}{27\sqrt{3}}\left[\frac{h^2+k^2+l^2}{(h^2+k^2+l^2)^2} - 3/5\right]\int_0^\infty r^4\exp(-\alpha r)\,j_4(4\pi sr)\;\mathrm{d}r. \tag{8}$$

These formulae are obtained by assigning a Slater-type function $r^n\exp(-\alpha r)$ with $n = 4$ to the radial part of the wave functions. The scaling constant κ_{nl}, exponential coefficient α, and the occupation numbers O and H are fitting parameters in this multipole model. By applying this model to both the experimental and the theoretical structure factors, we obtain the results shown in table 5. The MCDF atomic scattering factors are used in equation (6) for the experimental charge density, while the GGA and LDA 'atoms' are used for the corresponding LAPW charge densities. The free adjustable parameters here are the scaling

constants for the L and M shells, O, H and α. The Debye–Waller factor and the scaling of the L shell were found to be highly correlated for the experimental data. To avoid this, the Debye–Waller factor is fixed at 0.4668 Å^2 as obtained from the measurement with high-order reflections only. The use of atomic silicon scattering factors for the determination of the Debye–Waller factor from high-order structure factors is justified, since the theoretical calculations predict only a very small expansion of the L shell. The scaling of the L shell for the LAPW structure factors (for both GGA and LDA) as obtained from the multipole model analysis is opposite to the directly determined scaling (see the previous section). In the multipole model the scaling of the L shell is used to compensate for the deficiencies of the model, such as it not being possible to describe the charge modulation in the core region of the theoretical valence charge densities. The M-shell scaling factor shown in table 5 is also lower than reported previously [1, 23] on the basis of a smaller data set than that used here. The M-shell scaling in the multipole model for silicon was found to depend on the number of structure factors included in the refinement [9]. As the number of reflections included in the fit increases from 18 for the CH data set to 31, the scaling of the M shell changes from negative ∼4.2% (expansion) to positive 1.2% (contraction) for the LDA charge density [9]. This results from the reduced weight of low-order structure factors in the refinement. Such dependence highlights the deficiency of the multipole model, and raises questions about the significance of the individual fitting parameters. The residual of the model fit for the LDA is plotted in figure 8, showing that substantial systematic differences remain. The R-factor of the fit to the theoretical static charge density is of the same order of magnitude as the best agreement between theory and experiment.

Table 5. Parameters of the multipole model fitting. For details, see the text.

	k (L shell)	k (M shell)	O	H	α	R-factor
Experiment	0.9998(5)	0.971(8)	0.37(2)	−0.14(2)	4.76(10)	0.146%
LDA	1.0013	0.970	0.340	−0.0794	4.70	0.093%
GGA (PW91)	1.0013	0.967	0.355	−0.0841	4.67	0.094%

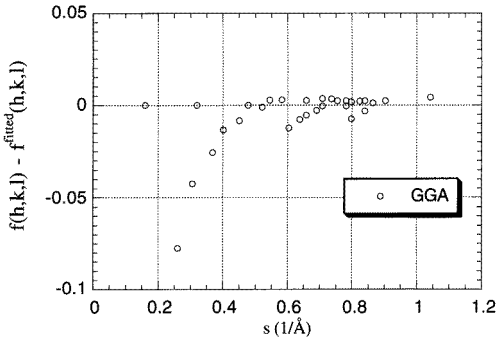

Figure 8. The form factor difference between the fitted and theoretical scattering factors of the LAPW method obtained using the PW91-GGA.

For relative comparisons, the M-shell scaling and the model parameters for the third-order Kubic harmonics terms are found to be very similar for the theoretical and experimental charge densities. The main difference lies in the L-shell scaling and the coefficient for the

fourth-order term, where the former is probably due to the modulation of charge density in the core region in the theoretical LAPW charge density, as discussed before. The anti-centrosymmetric third-order term transfers charge from an anti-bonding to a bonding region. The fourth-order term removes charge from the ⟨100⟩ to the ⟨111⟩ direction, enhancing the Si–Si bond and reducing the variations in the anti-bonding region [35]. The results of table 5 indicate that the experimental charge density contains a stronger fourth-order term than theory, which is evident from the stronger Si–Si bond found in the experimental data.

7. Effects of anharmonic vibration

The problem of anharmonic thermal vibration has been mentioned in section 2. Here we will discuss whether there is any evidence of anharmonic thermal vibration in the experimental structure factors of table 1. In the isolated-atom treatment of anharmonicity [27], the anharmonic thermal vibration of the Kubic term is given by

$$T_a = T_h\left(\frac{2\pi}{\gamma a_0}\right)^3 (K_B T)^2 \beta hkl \tag{9}$$

with $T_h = \exp(2\pi^2 K_B T g^2/\gamma)$ as the harmonic temperature factor. The anharmonic term vanishes for those reflections where one of the (h, k, l) indices is equal to 0 and for those satisfying $h + k + l = 4n$. Anharmonic vibrations have the largest effects on (555) among the reflections included in table 1. Figure 9 shows the effect of anharmonicity on the MCDF scattering factor with $\beta = 3.38$ eV Å^{-3}. The arrows are drawn only for those reflections with a relatively large correction term. With the exception of the case for (553), all of these 'corrections' worsen the agreement with experiment. From the theoretical calculation, we expect that crystal bonding will cause a change in the structure factor of high-order reflections, such as (555) and (753), of less than 5×10^{-3} electrons/atom. Taking this estimate into consideration, the magnitude of the change of the (555) and (753) reflections due to anharmonicity pushes them far outside the experimental error bar. Thus the measured x-ray structure factors indicate a much smaller β-value, in agreement with [23]. Neutron and x-ray measurements by Batterman and co-workers [39] give a low bound of $\beta = 1.38$ eV Å^{-3}; this results in an anharmonic term of about 6×10^{-3} electrons/atom for the (555) reflection, which is of the same order of magnitude as the change in high-order structure factors due to the crystal bonding. Therefore the determination of the anharmonicity from measured room

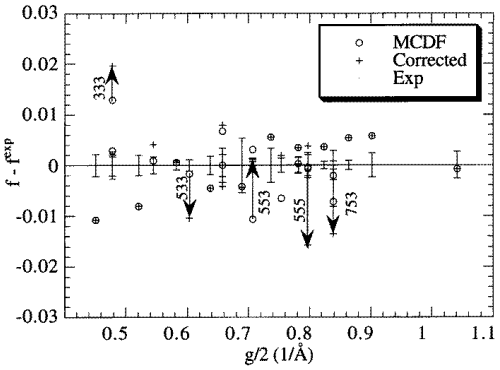

Figure 9. Effects of anharmonic thermal vibrations on the scattering factors with $\beta = 3.38$ eV Å^{-3}. The MCDF theoretical model is used for illustration.

temperature structure factors requires a better theoretical model for the high-order structure factors, which currently is not available. It is also obvious that the small upper limit of the anharmonic effects does not alter our previous comparisons in a significant way.

8. Discussion

The structure factors of high-order reflections are dominated by the contributions from the core electrons. Comparison between the experimental and theoretical structure factors of reflection (440) and higher shows that the best agreement is obtained with the Hartree–Fock approximations. Among the atomic models, the newly calculated atomic charge density of the MCDF method seems to be the best, but the difference between these MCDF results and the relativistic Hartree–Fock results of Doyle and Turner, as listed in the *International Tables for Crystallography*, is small. The experimentally determined Debye–Waller factor of Si depends on the atomic charge density used. For instance, using the non-relativistic HF densities of Clementi and Roetti results in a significantly lower Debye–Waller factor.

The highest accuracy of atomic charge densities is probably that given by the MCDF densities. We find a significant difference between these orbital densities and DS densities obtained within the LDA. The differences are reduced by using GGAs. The PW91-GGA gives a small but significant improvement for all orbital densities. The GGA of Engel and Vosko, which sacrifices the accuracy of the exchange energy for a better description of the exchange potential, yields even more accurate core densities, but for the valence states the EV-GGA is even worse than LDA. A new functional combining both the advantages of the EV-GGA in the core region and the better valence electron description in the PW91-GGA would be highly desirable.

Both the experimental and the theoretical charge-density difference maps clearly show the covalent bond of silicon. The overall bonding distribution has an oval shape. The bonding peak is slightly elongated along the bond in the experimental map, while the LAPW map has a more symmetric bonding peak. This is due to a larger fourth-order Kubic harmonic term in the experimental charge density, as found in the multipole model refinement. The theoretical LAPW map also shows a nodal-type modulation of valence electrons in the core region. A χ^2-test shows that this modulation of the structure factors is too small to be detected with the current experimental accuracy. It should be noted that this modulation is not present in the calculated difference map (figure 2(c) of Pisani *et al* [11]) in the HF-LCAO method. However, it is not clear whether the difference is due to the approximations for the exchange and correlation potential or the basis functions in these two methods. The chemical significance of a valence charge modulation in the core region, if it does exist, is not yet clear, but may be the result of orthogonalization to slightly modulated core wave functions. The traditional picture of chemical bonding involves the redistribution of outer valence electrons. Experimentally, this type of change in the core region is very difficult to detect even with improved accuracy because of the thermal vibrations. The scaling of the electron density in the core region and the determination of the Debye–Waller factor are highly correlated, and thus it is difficult to separate them. The effect of crystal bonding as predicted by LAPW-LDA and GGA (PW91) calculations is very similar, as can be seen from the difference maps of figure 5.

Figure 10 plots the form factor difference $\Delta f = f^{\text{crystal}} - f^{\text{atom}}$ between the crystal and the atom for both of the GGAs (PW91 and EV) and the LDA. The PW91-GGA and the LDA give similar values of Δf. This clearly shows that the difference in the structure factors between the GGA (PW91) and LDA comes from the atom. The GGA of Engel and Vosko gives a different Δf at low angles, especially for the lowest (111) reflection.

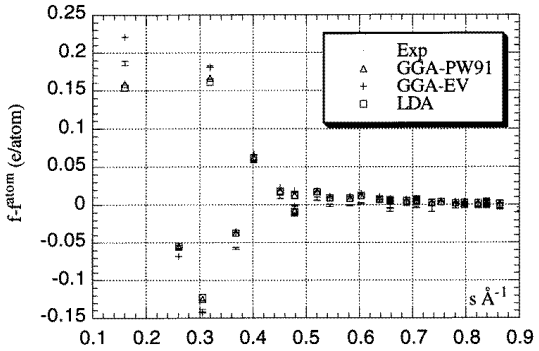

Figure 10. The form factor difference between the LAPW crystal and spherical atom for both of the GGAs and the LDA.

For the experimental Δf, the atomic reference of the MCDF [17] was used. The largest difference between this, the MCDF of Wang *et al* [19] and the configuration interaction of [20] is for the (111) structure factor (see table 1). Use of the latter two as atomic references will significantly reduce the value of Δf for the (111) reflection, and brings it closer to the GGA (PW91) and LDA values.

The charge density of silicon can be reasonably parametrized using a multipole model with an *R*-factor of about 0.15% for the experimental measurements. However, the significance of individual parameters is undermined by the ambiguity of separating a stationary crystal charge density, the residual systematic difference and the dependence of the parameters on the number of reflections included. In the multipole model refinement of the LAPW charge density, the scaling of the L-shell electrons shows a 0.13% contraction, while the direct comparison of charge densities indicates a 0.04% to 0.09% expansion of L-shell electrons. The scaling of M-shell electrons depends on the number of reflections included in the refinement, a fact first pointed out by Lu *et al* [9]. As the number of reflections included increases from 18 for the CH data set to 31, the scaling of the M shell changes from negative ∼4.2% (expansion) to positive 1.2% (contraction) [9]. A contraction of atoms in the crystal will lead to a smaller mean potential in the crystal, and is more consistent with the recent measurement of [21].

The best agreement with experimental structure factors is currently obtained with the LAPW method using the PW91-GGA [12] for exchange and correlation. The *R*-factor is about 0.13% and the GOF is about 8.8 using the averaged estimated standard error of 2.2×10^{-3} electrons/atom for the experimental scattering factors. The significance of the residual difference between theory and experiment depends on the experimental accuracy. There are a number of ways to estimate the experimental accuracy. One is from the scatter of the five measurements, which gives an averaged standard error of 4.7×10^{-3} electrons/atom. The standard errors listed in table 1 are the averaged estimated errors, which are calculated by considering the sources of error and their effects in the measurement, and indicate the precision of the measurement. Errors can also be estimated from the scatter of each reflection from the averaged value for a particular data set. Although the five sets of measurements were made by similar methods, the experimental details differ quite considerably. A better sense of the experimental accuracy would be given by the standard error of the latest Saka and Kato measurements, which is about 3.6×10^{-3} electrons/atom. Thus we have a lower and an upper limit of the averaged errors of 2.2 and 4.7×10^{-3} electrons/atom, respectively,

and the accuracy of the latest SK measurements falls in the middle. The GOFs of table 1 and 2 were calculated with the averaged standard error of 2.2×10^{-3} electrons/atom. If 3.6 or 4.7×10^{-3} electrons/atom are used, the best GOF drops to about 3.3 and 1.9, respectively. Either way, there is significant room for improvement in the agreement between theory and experiment.

9. Conclusions

From the study of the experimental and theoretical charge densities of silicon, we reach the following conclusions.

(i) The core electron densities are best described by atomic theories based on the (relativistic) Hartree–Fock approximation improved by extensive correlation treatments (e.g. the MCDF one). Within DFT, Engel and Vosko's version of the GGA for treating exchange and correlation effects comes closest. The GGA of Perdew and Wang, PW91, gives a better description than the LDA, but it is less accurate than the EV-GGA.

(ii) The GGA of Perdew and Wang, PW91, and the LDA give the best description of bonding, which is the redistribution of mostly valence electrons in crystals. However, the Engel–Vosko GGA deviates significantly.

(iii) It is desirable to find a density functional which combines the advantages of the GGA of EV for core electrons and the PW91-GGA for the valence electrons.

These conclusions are expected to remain valid for other systems. However, similar tests require highly accurate experimental structure factors to be available.

Acknowledgments

JMZ was supported by NSF grant 9412146, and thanks Dr P Rez for providing the MCDF atomic charge density of silicon, and Drs J C H Spence and M O'Keeffe for many discussions. PB was supported by the Austrian Science Foundation Project No P10847. We also thank the referees for highly constructive comments.

References

[1] Aldred P J E and Hart M 1973 *Proc. R. Soc.* A **332** 223
[2] Zuo J M, Spence J C H and O'Keeffe M 1988 *Phys. Rev. Lett.* **61** 353
Zuo J M 1993 *Acta Crystallogr.* A **49** 429
[3] Lu Z W and Zunger A 1992 *Acta Crystallogr.* A **48** 545
[4] Teworte R and Bonse U 1984 *Phys. Rev.* B **29** 2102
[5] Saka T and Kato N 1986 *Acta Crystallogr.* A **42** 469
[6] Saunders M and Bird D M 1995 *Ultramicroscopy* **60** 311
[7] Ren G, Zuo J M and Peng L M 1997 *Micron* at press
[8] Cumming S and Hart M 1988 *Aust. J. Phys.* **41** 423
[9] Lu Z W, Zunger A and Deutsch M 1993 *Phys. Rev.* B **47** 9385
[10] Spackman M A 1986 *Acta Crystallogr.* A **42** 271
[11] Pisani C, Dovesi R and Orlando R 1992 *Int. J. Quantum Chem.* **42** 5
[12] Perdew J P 1991 *Electronic Structure of Solids '91* ed P Ziesche and H Eschrig (Berlin: Akademie)
Perdew J P, Chevary J A, Vosko S H, Jackson K A, Pederson M R, Singh D J and Fiolhais C 1992 *Phys. Rev.* B **46** 6671
[13] Juan Y M and Kaxiras E 1992 *Phys. Rev.* B **48** 14 944
Garcia A, Elsasser C, Zhu J, Louie S G and Cohen M 1992 *Phys. Rev.* B **46** 9829
Filippi C, Singh D J and Umrigar C J 1994 *Phys. Rev.* B **50** 14 947

[14] Engel E and Vosko S H 1993 *Phys. Rev.* B **47** 13 164
[15] *International Tables for Crystallography* 1992 vol C (Dordrecht: Kluwer)
[16] Clementi E and Roetti C 1974 *At. Data Nucl. Data Tables* **14** 177
[17] Rez D and Rez P 1994 *Acta Crystallogr.* A **50** 481
[18] Grant I P, McKenzie B J, Norrington P H, Mayers D F and Pyper N C 1980 *Comput. Phys. Commun.* **21** 207
[19] Wang J, Sinth V H, Bunge C F and Jauregut R 1996 *Acta Crystallogr.* A **52** 649
[20] Meyer H, Muller T and Schweig A 1995 *Acta Crystallogr.* A **51** 171
[21] Gajdardziska-Josifovska M, McCartney M R, de Ruijter W J, Smith D, Weiss J K and Zuo J M 1993 *Ultramicroscopy* **50** 285
[22] O'Keeffe M and Spence J C H 1994 *Acta Crystallogr.* A **50** 33
[23] Deutsch M 1992 *Phys. Rev.* B **45** 646
[24] Alkire W, Yelon W B and Schneider J R 1982 *Phys. Rev.* B **26** 3097
[25] Deutsch M and Hart M 1988 *Phys. Rev.* B **37** 2701
[26] Zuo J M, Spence J C H and Hoier R 1989 *Phys. Rev. Lett.* **62** 547
[27] Willis T M and Pryor A W 1975 *Thermal Vibrations in Crystallography* (London: Cambridge University Press)
[28] Blaha P, Schwarz K, Dufek P and Augustyn R 1995 *WIEN 95* Technical University of Vienna
This is an improved and updated Unix version of the original copyrighted WIEN code, which was published by
Blaha P, Schwarz K, Sorantin P and Trickey S B 1990 *Comput. Phys. Commun.* **59** 399
[29] Schwarz K and Blaha P 1996 *Springer Lecture Notes in Chemistry* vol 67, ed C Pisani (Berlin: Springer) p 139
[30] Perdew J P and Wang Y 1992 *Phys. Rev.* B **45** 13 244
[31] Desclaux J P 1969 *Comput. Phys. Commun.* **1** 216
(The program used in this paper is a relativistic version of the published one.)
[32] O'Keeffe M 1993 private communication
[33] Wyckoff R W G 1963 *Crystal Structures* (Malabar, FL: Krieger)
[34] Maslen E N 1988 *Acta Crystallogr.* A **44** 33
[35] Dawson B 1967 *Proc. R. Soc.* A **298** 264
[36] Stewart R F 1973 *J. Chem. Phys.* **58** 1668
[37] Coppens P, Guru Row T N, Leung P, Stevens E D, Becker P J and Yang Y W 1979 *Acta Crystallogr.* A **35** 63
[38] Dufek P, Blaha P and Schwarz K 1994 *Phys. Rev.* B **50** 7279
[39] Roberto J B, Batterman B W and King D T 1974 *Phys. Rev.* B **9** 2590
Tischler J Z and Batterman B W 1984 *Phys. Rev.* B **30** 7060